Fault Detection and Identification on Pneumatic Production Machine

Barnabás Dobossy(✉), Martin Formánek, Petr Stastny, and Tomáš Spáčil

Brno University of Technology, Technická 2896, 616 69 Brno, Czech Republic
barnabas.dobossy@vutbr.cz

Abstract. Pneumatic cylinders have become integral parts of today's production machinery. In the age of just-in-time inventory system and with it the related production process, new, increased requirements were introduced. As a result, even the smallest fault in the system can lead to degradation in the product's quality in addition to this it can cause unplanned downtime leading to delays in production, not to mention higher costs. The availability of cheap sensors, big data, and algorithms from the field of predictive maintenance made the aforementioned problem tractable.

This paper examines whether signal-based condition indicators provide commercially viable and affordable basis for development of a health monitoring system for pneumatic actuator-based production machinery. The experiments and their results presented in this paper served two objectives. The first was to examine if faults on such equipment can be detected. The second was to identify the best combination of sensors, which are able to detect and identify fault with required accuracy. The evaluation of the sensors was not solely based on fault detection capabilities, but other practical aspects (price and durability of the sensors) were also taken into account.

Keywords: Health monitoring · Fault detection and isolation · Pneumatic cylinder · Production machinery

1 Introduction

Nowadays in the world of meticulously planned and timed production processes, even the smallest faults in production machinery can have serious consequences, leading to performance degradation, decrease in production, unplanned downtime, delays in production, problems with logistics not to mention safety hazards. Mechanical actuators, e.g. motors, hydraulic actuators, and pneumatic actuators are amongst the most vital parts of production machinery.

This research was funded by the Faculty of Mechanical Engineering, Brno University of Technology under the projects FSI-S-20-6407: "Research and development of methods for simulation, modelling a machine learning in mechatronics", and FV-21-03: "Laboratory model: Inertially driven inverse pendulum".

J. Mazal et al. (Eds.): MESAS 2021, LNCS 13207, pp. 39–60, 2022.
https://doi.org/10.1007/978-3-030-98260-7_3

This paper examines the applicability of state-of-the-art techniques for monitoring the evolution of the health conditions of pneumatic cylinders-based production machinery. The presupposition of these methods was affordability and increased accessibility of sensors which has led to the availability of big data and revolution of the maintenance procedure. A new approach called predictive maintenance has been developed which, contrary to the previously used techniques, introduced improvements in the field of condition monitoring, providing advancement in:

- fault detection and isolation (FDI),
- predicting the remaining useful life (the time interval in which the machine is expected to work as intended).

Condition monitoring is a term defining a group of methods that aim to evaluate the health of a system and its components by analysing and interpreting the data collected from the given system through sensors or transducers. Condition monitoring includes detection, isolation (diagnosis), and prediction of the faults in a system in the earliest possible stage. According to the definition of Prof. Rolf Isermann [1]: "A fault is unpermitted deviation of at least one characteristic property (feature) of the system from the acceptable, usual, standard condition". Eventually, it can result in loss or reduction of the capability to perform the required function and lead to failure and malfunction [1].

Fault detection and isolation deals with the detection of fault occurrence and pinpointing its source (location) in the system. Current applications of fault detection and identification systems are widespread, ranging from wind farms [2,3], electro-mechanical systems [6,12], pneumatic systems [4,5] up to machinery used for oil refinement in the petrochemical industry [13], or fault detection of sensors in a safety-critical control application [8].

Early fault detection methods were based on limit-checking of the monitored quantity, meaning the system is considered healthy if the monitored quantity Y lies between pre-defined upper and lower threshold values Y_{max} respectively Y_{min} [1]. Despite the method's simplicity, its significance was lost to condition indicator-based methods as the system's complexity increased.

Condition indicators are features of the data, that characterise the degradation process, meaning their value changes reliably and in a predictable manner as the system's health condition degrades. Due to their reliability, they are helpful in distinguishing healthy from faulty conditions, and they may even serve as a way to identify the source of the given faulty condition (e.g., excessive amount of vibration measured on a DC motor might suggest worn-out bearings) [19]. Generally, two main types of condition indicator are used:

- model-based condition indicator
- signal-based condition indicator

Of the two above-mentioned methods, the model-based condition indicators were the older approach [20]. The signal-based condition indicators were only developed in the 1980s as a result of technological advancements in the field of

digital signal processing. These new methods called signal-based methods were based on real-time processing of the measured signals which, included extraction and identification of properties or patterns within the signals that were correlated with changes in health conditions of the system, hence the name condition indicators. Deviation from the healthy values of the condition indicator is a sign of change in health conditions, which can be used to detect and identify different fault conditions.

The experiments in this paper on signal-based fault detection techniques will provide the foundation for the development of a commercially available health monitoring solution for pneumatic production machines. The planned solution should work as an early warning system by being able to detect faults before they would even occur, and warn the operators about their occurrence, and at the same time pinpoint their source. As a result, targeted maintenance action can be facilitated on the exact location of the fault at the right time, thus avoiding harm to the products or to the machine itself, saving expenses and making the manufacturing process more efficient. The application of the mathematical apparatus, and the algorithms in this paper is not only limited to pneumatic manufacturing equipment, but can be applied to other systems e.g., unmanned autonomous vehicles (UAV) with pneumatic suspensions, pneumatic break systems.

The paper examines, whether faults in pneumatic machines are detectable, identifiable and whether their source can be identified from analysis of sensor readings. The presented experiments will first and foremost concern the two most common sources of faults in real-life applications:

- faults of initial configuration of the machine (e.g. incorrect tuning of pressure level)
- faults emerging with usage of the machine as a result of wear

Several experiments were designed and performed to detect and identify these faults with the highest possible granularity, as well as to complete the following tasks:

- to identify the extent of detectability and identifiability of faults of a pneumatic actuator-based manufacturing machine from the available sensors
- to identify optimal sensor(s) that satisfy not just the precision requirements on condition monitoring but also requirements necessary for their deployment in a real-world industrial application, such as the following ones:
  - durability of the sensor (if possible, no mechanical parts)
  - no maintenance requirements
  - simple mounting
  - cost efficiency

A vital part of the signal-based approach is the extraction of the right condition indicators, from which the most expressive set of indicators can be selected for fault detection and isolation. A very powerful and popular group of condition indicators are features extracted from the frequency domain [3,4,12,15]. In [4]

the authors reached the conclusion that faults in pneumatic cylinders can be very well detected in the frequency domain of acoustic emission signal, while the emergence of new peaks in the frequency domain is correlated with faults in the system. In [15] authors successfully used frequency features of vibration signal successfully for health monitoring of bearings of DC motors.

Another popular source of condition indicators is the time-domain signal. In works [2] and [17] time-domain features such as kurtosis, crest factor, peak value, and RMS are used for health monitoring of a wind turbine. In [18] used similar time-domain condition indicators to detect faults in a gearbox. In [16] the author proposed a method, which exploited average time-domain vibration signal to detect health status changes of the gearbox.

The structure of this paper is as follows. Section 2 presents theoretical background with an emphasis on the workflow used and the processing steps carried out in each of its stages. Sections 3 and 4 describe the pneumatic testbench and the data acquisition signal chain used in the experiments. Section 3 takes a detailed look on the hardware, including the used sensors and adjustable parameters of the bench. Section 4 deals with the description of the data acquisition signal chain. The experiments and their results are presented in Sect. 5.

2 Signal-Based Condition Indicators

Keeping manufacturing machinery working effectively and minimising unavoidable downtime are two vital objectives in every production plant which are only achievable through a good maintenance strategy. Therefore maintenance timing is essential for efficient and cost-effective production. Based on the timing of the service intervention the following three maintenance strategies can be distinguished:

- *Reactive maintenance*:
  - the maintenance action takes place after a fault has already occurred
  - it is unexpected therefore the maintenance personnel cannot prepare for it
  - usually results in downtime of the machinery
- *Preventive maintenance*:
  - is carried out in fixed time intervals, regardless of whether the upkeep was needed
  - it was designed to keep parts in good condition
- *Predictive maintenance*:
  - the maintenance action is based on the analysis of information concerning the actual state of the machine
  - the upkeep action is targeted
  - it can be planned in advance
  - rarely results in a total shutdown of the whole factory
  - the parts are replaced right before a fault would occur, therefore their full lifetime is used

A more detailed description and comparison of the advantages and disadvantages of maintenance types is available in [7]. In the following section closer look on predictive maintenance workflow will be taken, while breaking the process up to its stages. In the following sections theoretical background will be explained in relations to the methodology used in our experiments.

3 Data Processing Workflow

The block diagram in Fig. 1 illustrates the main stages taken in the development of our fault detection and identification procedure. Contrary to the general predictive maintenance workflow which ends with implementation and deployment of the developed algorithm, this paper intends to serve only as a proof of concept of application of predictive maintenance for condition monitoring of a pneumatic actuator.

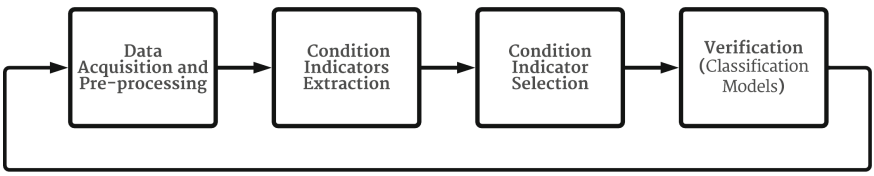

Fig. 1. Data processing workflow

In the following subsections, a detailed look at the individual stages of the above-presented workflow will be taken.

3.1 Data Acquisition and Pre-processing

Successful implementation of condition monitoring algorithms requires a data set of appropriate size and properties. The exact size of the data set is unknowable, therefore it has to be determined empirically, while taking into account the following properties also discussed in [9]:

- complexity of the problem
- complexity of the classification algorithm

It is also required for the used data set to include sufficient representation of the system's behaviour under a range of healthy and faulty conditions. This requirement is necessary in order to train a classifier with good generalisation properties. Further details on the parameters used to acquire data will be discussed in Sect. 5.1.

Pre-processing of the acquired data is the second stage in our workflow and it is an integral part of the process as the quality of the extracted condition indicator and also the accuracy of fault detection is dependent on the information content of the measured signal. Therefore, it is important to improve the quality

of the raw data by pre-processing it. Due to the high quality of sensors used and measurement hardware, the level of noise and other unwanted disturbances was acceptable, therefore pre-processing was limited only to the following operations:

- signals from the sensors were converted to physical quantities
- derivation of velocity and acceleration from the measured position data
- acquiring frequency domain representation of the signals through FFT

3.2 Condition Indicator Extraction

For the purpose of this paper MATLAB's Diagnostic Feature Designer was used to extract and select signal-based condition indicators from the measured signals. Signal-based condition indicators are the features of the signal, quantities that describe its behaviour, shape, frequency content and their value changes simultaneously with the system's degradation. They serve as a simple, computationally efficient, powerful, and reliable tools to produce features that can be used as condition indicators. The extracted features were from:

- time domain
- frequency domain

The application was used to generate a function to extract features. This function was later used to automate the feature extraction process and to produce features from the different measurements (Table 1).

Table 1. List of condition indicators extracted from the measured signals

List of condition indicators	
Domain	Condition indicator
Time-domain	Mean
	Standard deviation
	RMS
	Shape factor
	Kurtosis
	Skewness
	Peak value
	Crest factor
	Impulse factor
	Clearance factor
	Total harmonic distortion
	Signal-to-noise ratio
	SINAD
Frequency-domain	Peak amplitude
	Peak frequency
	Band power

3.3 Condition Indicator Selection

Feature selection is the fourth stage of the process. It is used to reduce the dimensionality of the feature space, which ranks and discards features that have bad predictive power. Feature selection is favourable because it improves the quality of the classification model, for the following reasons:

- prevents overfitting
- improves model size
- improves accuracy
- reduces training time

There is an abundance in various feature selection algorithms, the selection of which was made based on the findings of the paper [11]. The authors of the paper compared the performance of different selection algorithms on synthetic data, and the Relieff algorithm came out on top. In addition to the fact that this method belongs to the category of feature selection algorithms called filter methods (model with lowest computational cost), it performs well in rejecting correlated and redundant features and is not susceptible to non-linearity and noise of the features.

3.4 Verification of the Results

The fifth and final stage in our workflow was the verification of the chosen features, and simultaneously with it, the selection of sensors, i.e., sensor number reduction. To verify the fault detection quality of the sensors and their features, machine learning models were trained (no deep learning models) and the training results were validated using 6-fold cross-validation.

Table 2. Classifiers used during the verification procedure. In the column *Usage*, the letter *M* stands for multi-class classifier and *B* for binary classifier

Classification algorithms		
Family	Algorithm	Usage
Tree	Bagged	M
	Boosted	M
	Fine	B
	Medium	B
k-Nearest Neighbour	Fine	B/M
	Medium	B/M
	Weighted	B/M
Support Vector Machine	Cubic	M
	Medium Gaussian	M
	Quadratic	M
Discriminant Analysis	Subspace	M

The performed experiments from the perspective of how the classification problem is posed (i.e., number of classes) are of two kinds, binary and multi-class classification problems. Therefore suitable classifiers had to be chosen - 11 different classification models overall. The selected models are the best performing classifier models based on earlier experiments on the test data set. The selected algorithms are from 4 basic families of classifiers, ranging from Tree and Support Vector Machine to k-Nearest Neighbour and Discriminant analysis. The complete list of classifiers is available in Table 2.

The trained classification models were then tested by a cross-validation algorithm. Eventually, these results served as an indicator of the quality of the sensor and were used to pick the best combination of sensors that will be used during the further stages of our research and development activity.

MATLAB's Classification Learner application was used to train and test the machine learning models on the feature set.

4 Testbench Description

Data for the experiments was collected on a custom-built pneumatic device, which was designed and built to model the behaviour of pneumatic manufacturing equipment. The device has been developed to be able to model different stages of the manufacturing process (e.g., drilling, press-fit, etc.) and to mimic their behaviour not just under healthy conditions but also to simulate fault conditions.

In order to have versatile test equipment that can replicate accurately the behaviour of a pneumatic actuator under different production stages and also simulate fault condition, the testbench was designed to have adjustable parameters. The alterations can be made in:

- pressure of compressed air
- pressure reduction of the reduction valve
- the amount of the load acting on the cylinder (the platform's own weight is 7 kg)
- damping
  - both shock absorbers on two ends disengaged
  - both shock absorbers on both ends deployed
  - only one type of shock absorber on both ends is connected
    - with adjustable damping (9 levels of damping)
    - with constant damping

From the above-mentioned tuneable parameters the air pressure and the adjustments of the reduction valve are parameters, whose faults can occur from the negligence of the operator. While the other two parameters (e.g.: load, and damping) provide an easy way to replicate faults related to the manufacturing process (Fig. 2).

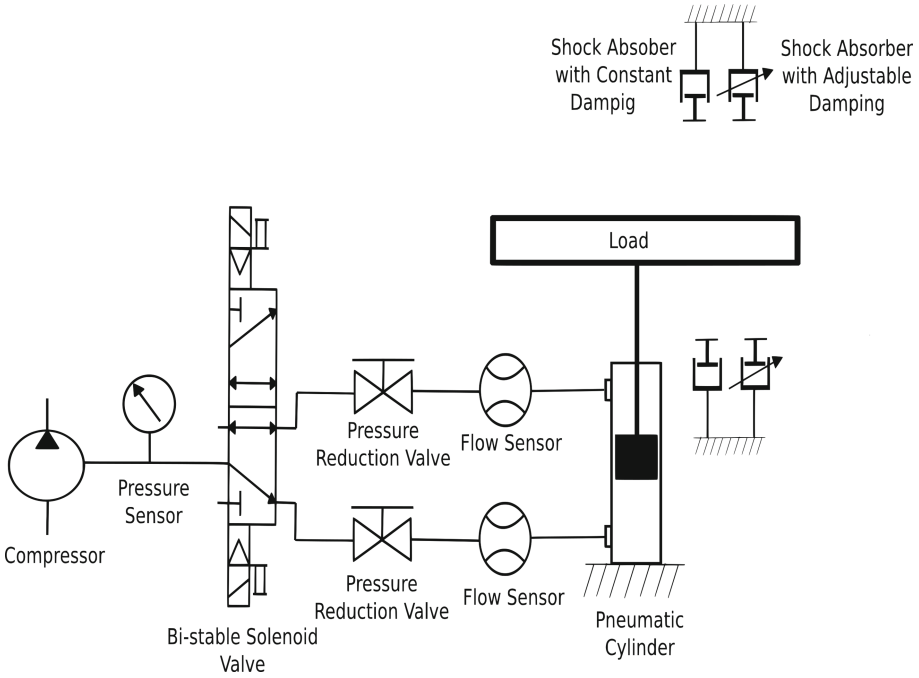

Fig. 2. Schematics of the pneumatic testbench

4.1 Sensors

Information on the motion and the state of the bench was obtained through a wide variety of sensors (8 types, 14 sensors altogether), in order to capture the most possible information, these sensors were mounted on different parts of the test bench (Fig. 3 and Fig. 4). Table 3 contains information regarding their type and the measured quantities:

Table 3. List of sensors mounted on the pneumatic test bench

List of sensors			
Code	Sensor type	Manufacture number	Range
S1	Accelerometer	TE Connectivity 4030-006-120	±6 g
S2	Flow sensor	Festo SFAB-50U-WQ6-2SV-M12	0–50 l/m
S3	Proximity switch	Festo SMT-8M-A-PS-24V-E-0.3-M8D	–
S4	Load cell	Burster 8524	0–2 kN
S5	Pressure sensor	Festo SDEI-D10-G2-MS-L-P1-M12	0–10 bar
S6	Microphone	VMA309	50–50 kHz
S7	Thermocouple	Omega SA2	−50–200 °C

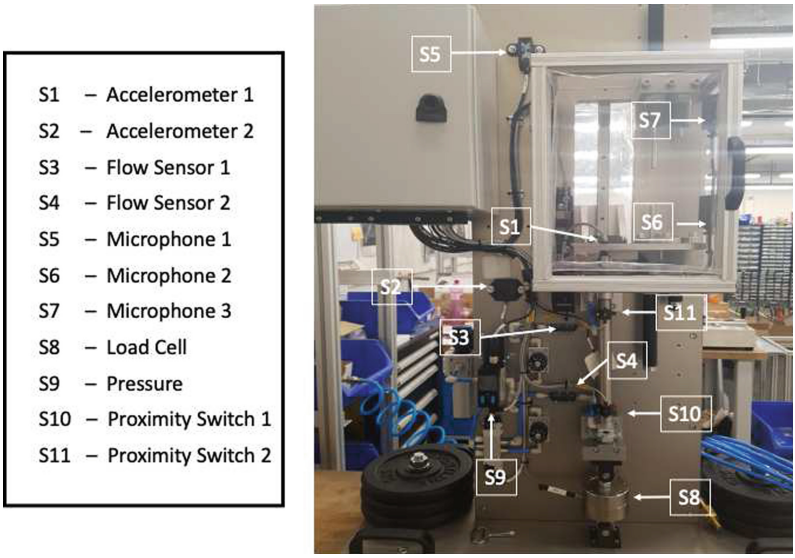

Fig. 3. Sensors of the test bench (front view)

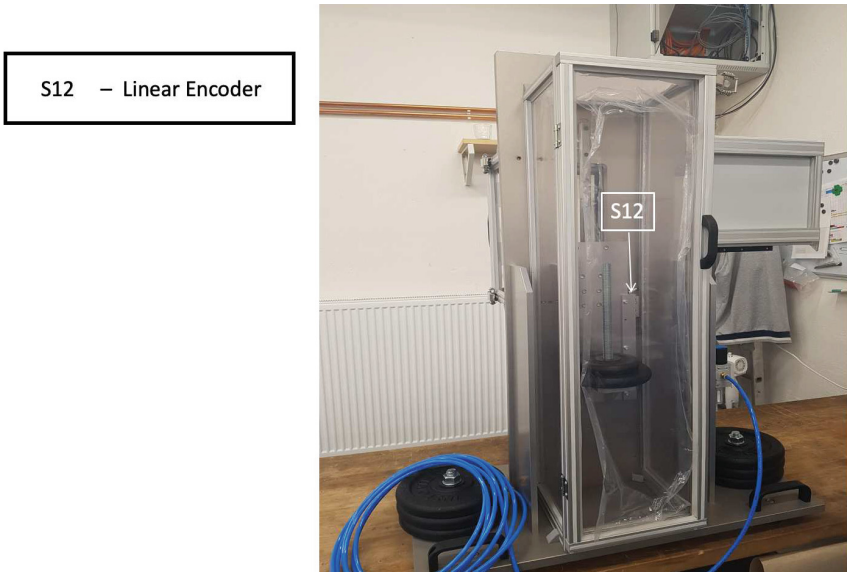

Fig. 4. Sensors of the test bench (rear view)

4.2 Reference Settings

Three common processes from automated manufacturing were chosen as the subjects of our experiment, namely:

- drilling
- assembly by press-fitting of parts
- transfer of assembled parts between workstations

Before the experiments could be carried out, the unknown values for the bench's adjustable parameters for the above-mentioned processes had to be identified. Altogether 7 different prescriptions for ideal working conditions were obtained (2x drilling, 2x assembly by press-fitting, 3x transfer). These settings will be used during the experiments as reference states (healthy conditions), since they define how the testbench should behave under normal operating conditions. The following table presents the mentioned healthy conditions:

Table 4. Healthy (reference) states of adjustable parameters of the pneumatic test bench

Operations		Transfer			Assembly		Drilling	
ID		11	12	13	21	22	31	32
Load [kg]		6,25	5	0	0	1,25	0	1,25
Pressure [bar]		6	6	6	6	6	5,5	6
Reduction valve 1		4	4	3	3	3	5	5
Reduction valve 2		2	2	3	3	3	3	3
Bottom shock absorber	Adjustable damping	4	4	3	3	3	5	5
	Constant damping	4	4	3	3	3	5	5

5 Data Acquisition

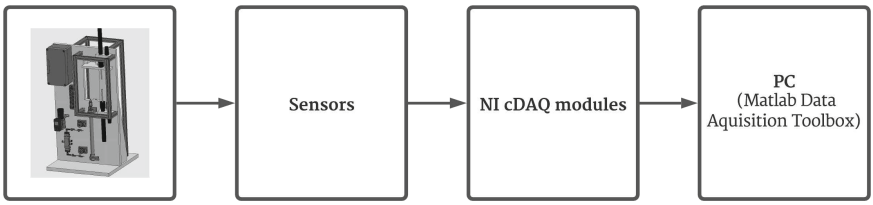

Fig. 5. Block diagram of the data acquisition signal chain

The block diagram in Fig. 5 presents the data acquisition signal chain used in our experiments. The used measurement chain consists of six NI cDAQ modules,

the complete list of modules, connection diagram, and sampling information are presented in Table 5. To control the timing and the data transfer from the individual modules, NI's cDAQ-9172 chassis was used.

In addition to the high slot count among other advantages of this chassis is the possibility of multi-rate sampling of the modules (3 objects each with its own sampling rate). This property was highly advantageous due to the fact that the measured quantities have different dynamics. Therefore, the measured signals were grouped into three groups based on their sampling rate. Three microphones were sampled at a rate of 40 kHz, the thermocouple at 0,1 Hz, and the rest of the sensors at 1 kHz.

Table 5. Connection diagram of the used test bench

Sensor type	HW	Signal type	Sampling rate [kHz]
Pressure sensor	NI 9221	Analog	1
Flow sensor	NI 9221	Analog	1
Accelerometer	NI 9221	Analog	1
Linear encoder	NI 9401	Analog	1
Load cell	NI 9211	Analog	1
Proximity sensor	NI 9411	Digital	1
Microphone	NI 9215	Analog	40
Thermocouple	NI 9419	Analog	0,1

5.1 Data Acquisition Firmware

The configuration of the data acquisition hardware and the data measurement session was controlled by MATLAB's Data Acquisition Toolbox, which provided a powerful yet simple-to-use environment to exploit the device specific features of the NI hardware. As it was mentioned above, due to the different nature of the measured quantities, multi-rate sampling was deemed an optimal technique to use. To utilise NI hardware's multi-rate functionality, three separate data acquisition objects ("daq") were created. Sensors through measurement channels were assigned to each of these objects according to the table above. The specificity of this multi-rate approach is that in order to trigger and synchronize the execution of the data acquisition objects one of them has to be selected as the master, while the rest of them are slave objects. Practically, it means that the master object is started manually with a run command from the MATLAB script and subsequently triggers the acquisition start of the slave objects. In addition to scripts that control the data acquisition, further conversion functions were created which convert the electrical quantities from the sensors to the given physical quantity of the measured signals. Lastly, a function converts the individual timetables with measurement data (each sensor has its own) to a large table, containing the measurements from the data acquisition objects to

a format suitable for further processing with the feature extractor application called Diagnostic Feature Designer - part of MATLAB's Predictive Maintenance Toolbox.

6 Experimental

Among the goals of this paper was to experimentally identify the extent to which faults can be detected and identified with sufficient detection accuracy. Therefore, experiments with increasing complexity were designed. Starting from detection of fault (distinguishing between healthy and faulty conditions) to identifying the source and the degree by which the faulty configuration is offset from the healthy conditions. The of experiments in execution order is presented below:

- **Single fault condition**
  1. Fault detection in one specific process
  2. Fault detection and isolation in one specific process
     a identification of the source of the fault
     b identification of the source (exact setting of the adjustable parameter)
- **Combination of two fault conditions**
  1. Fault detection and isolation in one specific process, where the combination of two fault conditions occur at the same time

The course of the experiments was identical in every case. With each setting of the adjustable parameters, 20 cycles (in our case a cycle consists of a full extrusion of the cylinder's rod and its return to its original position) worth of data was captured. The number of cycles was determined by taking into account two factors. The first of them was the selection of classification algorithms, which was constrained to supervised learning models not requiring deep learning. As result, there were fewer parameters to learn during the training of the classifier, and at the same time the training data set could be kept reasonable small. The second factor was know-how, collected from previous experiments on the testbench.

Each set of measurements for the given reference setting consisted of data representing both healthy and faulty conditions. The healthy conditions were the reference settings themselves (available in Table 4 while the faulty conditions were defined as any deviation of adjustable parameters from the prescribed reference settings.

7 Results

Table 6 displays the results of the first experiment for process 11 are displayed. As the results point out, the best fault detection accuracy is provided by the sensors such as linear encoder and microphone, where the accuracy reaches 100%. As for the other sensors the fault detection accuracy is very high as well (greater than 90%). The other processes showed similar results to the ones presented in Table 6 (Fig. 6).

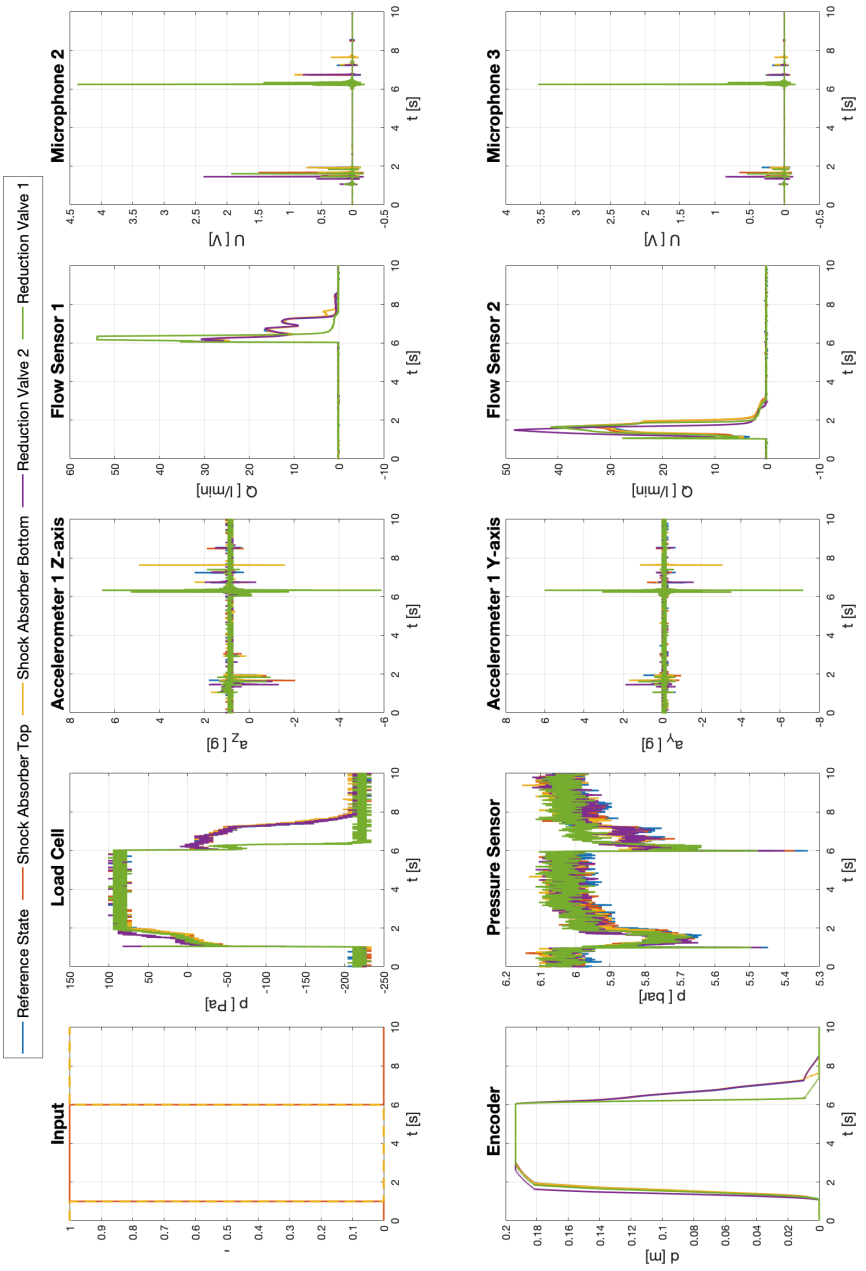

Fig. 6. Illustration of measured signals for each of the examined health conditions

Table 6. Classification results of single-fault fault detection. In column *Acc.* the classification accuracy is presented in percentage and in column *Classifier*, the name of the best performing classifier model's name is displayed.

Transfer between stages		
Sensor	11	
	Acc.	Classifier
Accelerometer 1 Y-axis	99.6	Fine KNN
Accelerometer 1 Z-axis	98.2	Weigh. KNN
Accelerometer 2 Y-axis	95.6	Bagged Tree
Accelerometer 2 Z-axis	93.3	Medium Tree
Encoder	100	Fine KNN
Flow Sensor 1	99.7	Fine KNN
Flow Sensor 2	99.4	Fine KNN
Microphone 1	97.3	Fine KNN
Microphone 2	99.9	Weight. SVN
Microphone 3	100	Fine KNN
Load Cell	99.4	Fine Tree
Pressure	90.8	Boost. Tree

Based on the results, it can be concluded that all of the available sensors passed the first test and can undergo further investigation in order to find the extent to which these sensors are suitable for a more complex tasks.

Table 7. Classification results of single-fault fault detection and isolation for the process transfer between stages. In column *Acc.* the classification accuracy is presented in percentage and in column *Classifier*, the name of the best performing classifier model's name is displayed.

Transfer between stages						
Sensor	11		12		13	
	Acc.	Classifier	Acc.	Classifier	Acc.	Classifier
Accelerometer 1 Y-axis	98.9	Quadr. SVM	93.3	Cubic SVM	98.6	Gauss. SVM
Accelerometer 1 Z-axis	92.9	Weigh. KNN	91.8	Weigh. KNN	94.7	Quadr. SVM
Accelerometer 2 Y-axis	93.9	Quadr. SVM	82.3	Boost. Tree	85.8	Bagged Tree
Accelerometer 2 Z-axis	91.4	Quadr. SVM	87.0	Boosted Tree	95.8	Cubic SVM
Encoder	99,6	Fine KNN	99.9	Fine KNN	100	Fine KNN
Flow Sensor 1	99.4	Quadr. SVM	99.9	Cubic SVM	98.8	Cubic SVM
Flow Sensor 2	98.5	Quadr. SVM	99.1	Cubic SVM	94.6	Bagged Tree
Microphone 1	95.8	Quadr. SVM	82.4	Bagged Tree	88.5	Bagged Tree
Microphone 2	93.6	Quadr. SVM	93.3	Bagged Tree	94.0	Boosted Tree
Microphone 3	90.8	Bagged Tree	91.8	Boosted Tree	92.2	Boost. Tree
Load Cell	99.1	Quadr. SVM	98.8	Quadr. SVM	98.8	Bagged Tree
Pressure	80.6	Weigh. KNN	78.5	Quadr. SVM	87.5	Boosted Tree

In the case of the next experiment (Tables 7, 8 and 9), the fault detection and identification capabilities of the sensors were tested. This time just like in the case of the previous experiment only a single fault condition was modeled (only one adjustable parameter was changed against the reference states) at a time.

Table 8. Classification results of single-fault fault detection and isolation for the process assembly by press-fitting. In column *Acc.* the classification accuracy is presented in percentage and in column *Classifier*, the name of the best performing classifier model's name is displayed.

Assembly by press-fitting				
Sensor	21		22	
	Acc.	Classifier	Acc.	Classifier
Accelerometer 1 Y-axis	81.0	Cubic SVM	81.8	Gauss. SVM
Accelerometer 1 Z-axis	90.6	Quadr. KNN	87.9	Weigh. KNN
Accelerometer 2 Y-axis	73.8	Boost. Tree	82.6	Gauss. SVM
Accelerometer 2 Z-axis	76.8	Quadr. SVM	85.6	Quadr. SVM
Encoder	99,4	Cubic SVN	99.7	Fine KNN
Flow Sensor 1	97.7	Quadr. SVM	100	Cubic SVM
Flow Sensor 2	98.2	Quadr. SVM	99.9	Fine KNN
Microphone 1	84.3	Quadr. SVM	85.3	Boosted Tree
Microphone 2	84.0	Weigh. SVM	81.1	Quadr. SVM
Microphone 3	89.9	Quadr. SVM	88.5	Quadr. SVM
Load Cell	93.2	Bagged Tree	98.0	Cubic SVM
Pressure	63.2	Boost. Tree	88.0	Weigh. KNN

As a result of the higher requirements on the desired output, the classifier had to distinguish more nuanced differences within the data in order to identify the source of the fault.

Table 9. Classification results of single-fault fault detection and isolation for the process drilling. In column *Acc.* the classification accuracy is presented in percentage and in column *Classifier*, the name of the best performing classifier model's name is displayed.

Drilling				
Sensor	31		32	
	Acc.	Classifier	Acc.	Classifier
Accelerometer 1 Y-axis	62.4	Boosted Tree	62.3	Quadr. SVM
Accelerometer 1 Z-axis	84.8	Bagged Tree	85.6	Quadr. SVM
Accelerometer 2 Y-axis	44.1	Med. KNN	46.5	Quadr. SVM
Accelerometer 2 Z-axis	52.1	Quadr. SVM	48.2	Quadr. SVM
Encoder	98.5	Quadr. SVM	99.1	Quadr. SVM
Flow Sensor 1	99.5	Quadr. SVM	95.2	Cubic. SVM
Flow Sensor 2	96.3	Bagged Tree	98.5	Weigh. SVM
Microphone 1	88.4	Boosted Tree	81.8	Cubic SVM
Microphone 2	94.1	Boosted Tree	91.2	Quadr. SVM
Microphone 3	94.8	Bagged Tree	90.3	Bagged Tree
Load Cell	99.3	Quadr. SVM	99.2	Quadr. SVM
Pressure	82.4	Weigh. SVM	85.9	Quadr. SVM

Table 10. Single-fault detection and isolation (with identification of the exact settings) for the process transfer between stages. In column *Acc.* the classification accuracy is presented in percentage and in column *Classifier*, the name of the best performing classifier model's name is displayed.

Transfer between stages						
Sensor	11		12		13	
	Acc.	Classifier	Acc.	Classifier	Acc.	Classifier
Accelerometer 1 Y-axis	83.5	SubSp. Disc	81.7	Cubic SVM	81.0	SubSp. Disc.
Accelerometer 1 Z-axis	80.8	Cubic SVM	78.3	Quadr. SVM	83.5	SubSp. Disc.
Accelerometer 2 Y-axis	70.6	SubSp. Disc	68.5	Bagged. Tree	57.3	Gauss. SVM
Accelerometer 2 Z-axis	63.0	Gauss. SVM	61.8	Bagged Tree	67.7	Gauss. SVM
Encoder	96.5	Cubic SVM	99.1	Fine KNN	100	Fine KNN
Flow Sensor 1	99.6	Cubic SVM	93.2	Quadr. SVM	93.0	SubSp. Disc.
Flow Sensor 2	88.9	Quadr. SVM	92.9	SubSp. Disc	88.8	Quadr. SVM
Microphone 1	80.6	Gauss. SVM	70.0	Bagged Tree	72.2	Quadr. SVM
Microphone 2	80.8	Cubic KNN	86.4	Quadr. SVM	83.3	Quadr. SVM
Microphone 3	80.6	Gauss. SVM	85.8	Quadr. SVM	84.8	Cubic SVM
Load Cell	91.7	Quadr. SVM	92.7	Bagged Tree	92.5	Bagged Tree
Pressure	63.0	Quadr. SVM	64.1	Bagged Tree	66.7	SubSp. Disc

As expected, the more refined differences in data made the classifiers work complex, which resulted in decreased classification performance in case of every used sensor. The biggest decrease in performance (50%), in comparison to the first experiment, occurred in the case of the accelerometer fixed to the frame of the test bench.

Table 11. Single-fault detection and isolation (with identification of the exact settings) for the process assembly by press-fitting. In column *Acc.* the classification accuracy is presented in percentage and in column *Classifier*, the name of the best performing classifier model's name is displayed.

Assembly by press-fitting				
Sensor	21		22	
	Acc.	Classifier	Acc.	Classifier
Accelerometer 1 Y-axis	57.9	SubSp. Disc	49.9	SubSc. Disc.
Accelerometer 1 Z-axis	75.0	SubSc. Disc	67.1	SubSc. Disc.
Accelerometer 2 Y-axis	41.4	SubSc. Disc	46.2	SubSc. Disc.
Accelerometer 2 Z-axis	39.9	SubSc. Disc	45.3	SubSc. Disc.
Encoder	99,4	Cubic SVN	98.9	Quadr. SVM
Flow Sensor 1	92.5	Quadr. SVM	97.0	Cubic SVM
Flow Sensor 2	94.0	SubSp. Disc	95.0	SubSc. Disc.
Microphone 1	62.2	Bagged Tree	58.8	Bagged Tree
Microphone 2	59.12	Quadr. SVM	61.2	Quadr. SVM
Microphone 3	66.8	Quadr. SVM	69.1	Quadr. SVM
Load Cell	87.5	Cubic SVM	98.9	Quadr. SVM
Pressure	61.0	SubSp. Disc	75.0	SubSc. Disc

Table 12. Single-fault detection and isolation (with identification of the exact settings) for the process drilling. In the column *Acc.* the classification accuracy is presented in percentage and in column *Classifier*, the name of the best performing classifier model's name is displayed.

Drilling				
Sensor	31		32	
	Acc	Classifier	Acc	Classifier
Accelerometer 1 Y-axis	43.6	Quadr. SVM	37.2	Quadr. SVM
Accelerometer 1 Z-axis	61.9	Quadr. SVM	55.7	Cubic SVM
Accelerometer 2 Y-axis	26.7	SubSp. Disc	23.8	Gauss. SVM
Accelerometer 2 Z-axis	30.5	Quadr. SVM	27.1	Gauss. SVM
Encoder	98.6	Cubic SVM	94.6	Quadr. SVN
Flow Sensor 1	90.5	SubSp. Disc	92.7	Quadr. SVM
Flow Sensor 2	92.4	SubSp. Disc	87.4	Cubic SVM
Microphone 1	66.7	Quadr. SVM	61.8	Quadr. SVM
Microphone 2	84.7	Quadr. SVM	79.2	Quadr. SVM
Microphone 3	82.2	Quadr. Tree	76.4	Quadr. SVM
Load Cell	92.9	Bagged Tree	94.7	Quadr. SVM
Pressure	77.1	Weigh. SVM	62.3	Quadr. SVM

In the case of the other sensors, the drop in performance was less significant. Among the best performing sensors were the linear encoder, both flow sensors, load cell, and the accelerometer mounted on the moving part that lifts the weights. The accuracy of these sensors was above 90%.

Another interesting fact is that the condition indicators from processes such as drilling and assembly by press-fitting turned out to be harder to detect.

Table 13. Classification accuracy for detection and isolation of combination of two faults. In the column *Acc.* the classification accuracy is presented in percentage and in column *Classifier*, the name of the best performing classifier model's name is displayed.

Assembly by press-fitting		
Sensor	32	
	Acc.	Classifier
Accelerometer 1 Y-axis	84.0	Cubic SVM
Accelerometer 1 Z-axis	80.1	Quadr. SVM
Accelerometer 2 Y-axis	59.4	Bagged Tree
Accelerometer 2 Z-axis	59.3	Bagged Tree
Encoder	99.2	Cubic SVM
Flow Sensor 1	95.5	Quadr. SVM
Flow Sensor 2	94.4	Cubic SVM
Microphone 1	66.7	Bagged Tree
Microphone 2	84.8	Bagged Tree
Microphone 3	84.0	Bagged Tree
Load Cell	94.3	Bagged Tree
Pressure	67.0	Bagged Tree

In the last experiment which dealt with the detection and identification of a single fault, the goal of the experiment was to detect and identify faults to the extent in which the classifier can tell not just the exact source of the fault, but also how much the current setting differs from the reference setting, e.g., in the case of reference state 11, the *Reduction* Valve 1 was set to position 9 instead of 4. In this case, an overall slight worsening of accuracy is noticeable (Tables 10, 11 and 12). Sensors such as the linear encoder, load cell, and both flow sensors are still providing results with over 90% accuracy, however, the rest of the sensors have inferior capabilities to detect faults with such detailedness.

The last experiment was designed to detect fault detection and isolation capabilities of the sensors for the combination of two fault conditions occurring at the same time. In this experiment, the results (Table 13) were the same as in the case of experiment number 3. The best overall performance was obtained from the features from sensors such as the linear encoder, load cell, and both flow sensors. The encoder was the best by significant margin, reaching 99.2% accuracy.

In each case where classification is discussed, it is vital to mention the stability of the results after multiple re-training of the classifier models. The overall fluctuation in the results of classification accuracy was around 2–3%, while in the case of the encoder, the stability of the results was even greater around 0.1 percentage points.

By considering factors, namely cost and practicality related to the use and mounting of the sensor, there is a slight alteration in the end result (Table 14). Sensors such as flow sensor and load cell become impractical. In the case of the load cell, it is due to its cost and problematic mounting. Based on the results above, it is clear that condition indicators from encoders provide incomparable classification performance despite their relatively high cost. Accelerometers are not suited for detection of the degree by which the fault condition of the machinery differs from the ideal state, however, they make up for it in the other two vital perspectives.

Table 14. Comparison of the four best sensors based on classification accuracy (*Accuracy*), price *Cost*, and ease of usage and application Practicality

Sensor	Accuracy	Cost	Practicality
Linear encoder	⋆⋆⋆⋆⋆	⋆⋆	⋆⋆
Flow sensor	⋆⋆⋆⋆⋆	⋆⋆⋆	⋆
Accelerometer	⋆⋆⋆	⋆⋆⋆⋆	⋆⋆⋆⋆⋆
Load cell	⋆⋆⋆⋆⋆	⋆	⋆

8 Conclusion

The main contribution of our work is proof showing that signal-based condition indicators are a viable approach to monitor the health condition and to detect and identify faults in the case of pneumatic actuator-based production machines. The presented methods can be further applied to a variety of pneumatic systems e.g., suspension of UAVs, break systems.

Based on the presented results from the previous section, it can be concluded that condition indicators from sensors, such as the encoder, flow sensor, or load cell are capable of identifying even the degree by which the fault condition of the machinery differs from the ideal, healthy state of the machine. It was also shown that condition indicators from these sensors are capable of detecting single fault and also the combination of two faults, which occur at the same time. In the case of reduced requirements, which only require identification of the source of the fault, the accelerometer mounted onto the moving part of the machine can be a viable option.

Inclusion of other aspects to our evaluation such as practicality or the cost of the sensors changes the end result. Based on the new evaluation criterion, the encoder will become the single best sensor for all of the examined tasks.

However, if we are satisfied only with the identification of the source of the fault, accelerometer is an obvious choice due to its low cost and ease of usage.

Acknowledgment. We would like to thank Mechatronic Design Solution ltd. for their help in designing and building the pneumatic test bench and for their expertise with pneumatic actuator-based production machinery.

References

1. Isermann, R.: Fault-Diagnosis Systems: An Introduction from Fault Detection to Fault Tolerance. Springer, Berlin (2006)
2. Hu, A., Xiang, L., Zhu, L.: An engineering condition indicator for condition monitoring of wind turbine bearings. Wind Energy (Chichester, England) **23**, 207–219 (2020). https://doi.org/10.1002/we.2423
3. Yang, W., Tavner, P.J., Crabtree, C.J., Wilkinson, M.: Cost-effective condition monitoring for wind turbines. IEEE Trans. Ind. Electron. **57**, 263–271 (2010). https://doi.org/10.1109/TIE.2009.2032202
4. Mahmoud, H., Mazal, P., Vlašic, F.: Detecting pneumatic actuator leakage using acoustic emission monitoring. Insight (Northampton) **62**, 22–26 (2020). https://doi.org/10.1784/insi.2020.62.1.22
5. Dunbar, W.B., de Callafon, R.A., Kosmatka, J.B.: Coulomb and viscous friction fault detection with application to a pneumatic actuator. In: 2001 IEEE/ASME International Conference on Advanced Intelligent Mechatronics. Proceedings (Cat. No. 01TH8556), vol. 2, pp. 1239–1244. IEEE (2001). https://doi.org/10.1109/AIM.2001.936889
6. Pandhare, V., Singh, J., Lee, J.: Convolutional neural network based rolling-element bearing fault diagnosis for naturally occurring and progressing defects using time-frequency domain features. In: 2019 Prognostics and System Health Management Conference (PHM-Paris), pp. 320–326. IEEE (2019). https://doi.org/10.1109/PHM-Paris.2019.00061
7. Lacey, J.: The Role of Vibration Monitoring in Predictive Maintenance. https://www.schaeffler.com/remotemedien/media/_shared_media/08_media_library/01_publications/schaeffler_2/technicalpaper_1/download_1/the_role_of_vibration_monitoring.pdf
8. Grepl, R., Matejasko, M., Bastl, M., Zouhar, F.: Design of a fault tolerant redundant control for electro mechanical drive system. In: 2015 21st International Conference on Automation and Computing (ICAC), pp. 1–6. Chinese Automation and Computing Society in the UK - CACS (2015). https://doi.org/10.1109/IConAC.2015.7313984
9. Brownlee, J.: How Much Training Data is Required for Machine Learning? www.machinelearningmastery.com/much-training-data-required-machine-learning/
10. Data Preprocessing for Condition Monitoring and Predictive Maintenance. www.mathworks.com/help/predmaint/ug/data-preprocessing-for-condition-monitoring-and-predictive-maintenance.html
11. Bolón-Canedo, V., Sánchez-Maroño, N., Alonso-Betanzos, A.: A review of feature selection methods on synthetic data. Knowl. Inf. Syst. **34**, 483–519 (2013)
12. Bouzida, A., Touhami, O., Ibtiouen, R., Belouchrani, A., Fadel, M., Rezzoug, A.: Fault diagnosis in industrial induction machines through discrete wavelet transform. IEEE Trans. Ind. Electron. **58**, 4385–4395 (2011). https://doi.org/10.1109/TIE.2010.2095391

13. Zhang, Y., Jiang, J., Flatley, M., Hill, B.: Condition monitoring and fault detection of a compressor using signal processing techniques. In: Proceedings of the 2001 American Control Conference (Cat. No. 01CH37148), vol. 6, pp. 4460–4465. IEEE (2001). https://doi.org/10.1109/ACC.2001.945681
14. Srividya, A., Verma, A.K., Sreejith, B.: Automated diagnosis of rolling element bearing defects using time-domain features and neural networks. Int. J. Min. Reclama. Environ. **23**, 206–215 (2009). https://doi.org/10.1080/17480930902916437
15. Abbasion, S., Rafsanjani, A., Farshidianfar, A., Irani, N.: Rolling element bearings multi-fault classification based on the wavelet denoising and support vector machine. Mech. Syst. Signal Process. **21**, 2933–2945 (2007). https://doi.org/10.1016/j.ymssp.2007.02.003
16. Mcfadden, P.D.: Examination of a technique for the early detection of failure in gears by signal processing of the time domain average of the meshing vibration. Mech. Syst. Signal Process. **1**, 173–183 (1987). https://doi.org/10.1016/0888-3270(87)90069-0
17. Zhu, J., Nostrand, T., Spiegel, C., Morton, B.: Survey of Condition Indicators for Condition Monitoring Systems (Open Access) (2014)
18. Večeř, P., Kreidl, M., Šmíd, R.: Condition indicators for gearbox condition monitoring systems. Acta polytechnica (Prague, Czech Republic: 1992) **45** (2005). https://doi.org/10.14311/782
19. Condition Indicators for Monitoring, Fault Detection, and Prediction. https://www.mathworks.com/help/predmaint/ug/condition-indicators-for-condition-monitoring-and-prediction.html
20. Dai, X., Gao, Z.: From model, signal to knowledge: a data-driven perspective of fault detection and diagnosis. IEEE Trans. Ind. Inform. **9**, 2226–2238 (2013). https://doi.org/10.1109/TII.2013.2243743